Gait & Posture 34 (2011) 462–466

Contents lists available at ScienceDirect

Gait & Posture

journal homepage: www.elsevier.com/locate/gaitpost

Ambulatory running speed estimation using an inertial sensor

Shuozhi Yang [a], Chris Mohr [b], Qingguo Li [a,c,*]

[a] Department of Mechanical and Materials Engineering, Queen's University, Kingston, ON, Canada
[b] Department of Mechanical Engineering, Royal Military College, Kingston, ON, Canada
[c] Human Mobility Research Centre, Queen's University and Kingston General Hospital, Kingston, ON, Canada

ARTICLE INFO

Article history:
Received 4 November 2010
Received in revised form 30 May 2011
Accepted 24 June 2011

Keywords:
Running speed
Ambulatory
Biomechanics
Inertial measurement unit
Gait segmentation

Abstract: Techniques have been developed to analyze walking gait using accelerometer and gyroscope data from miniature inertial measurement units (IMU), but few attempts have been made to use similar approaches for running gait. The purpose of this study was to develop an algorithm capable of estimating running speed using a single shank-mounted IMU. Raw acceleration and angular velocity were recorded from an IMU sensor attached on the lateral side of the shank in the sagittal plane and a method of reliably detecting the shank vertical and the minimal shank velocity gait event was used to segment a running sequence into individual strides. Through integration, the orientation of the shank segment was determined and an estimate of stride-by-stride running speed was calculated by integrating the acceleration data. The algorithm was verified using data collected from a group of seven volunteers running on a treadmill at speeds between 2.50 m/s and 3.50 m/s. Over the entire speed range, the estimation results gave a percentage root mean square error (%RMSE) of approximately 4.10%. With the accurate estimation capability and portability, the use of the proposed system in outdoor running gait analysis is promising.

1. Introduction

There is growing interest in the measurement of the mechanics of human locomotion (walk/running gait analysis) for clinical studies, rehabilitation, prosthetics development, sports training and personal fitness. Currently, the characteristics and kinematics of human gait are typically observed using optical methods (video cameras used in conjunction with passive or active markers attached to the subjects). These optical methods are expensive and are limited to in-lab testing due to the complex equipment settings and working space needed [1]. Thus, there is a potential demand for portable sensors that can estimate gait properties such as speed, stride length and stride frequency of an individual in non-laboratory environments, especially for the research on outdoor sports.

While the use of miniature inertial sensors, such as accelerometers and gyroscopes, in gait analysis is not new, many previous applications have been reported on using inertial sensors in estimating gait events or temporal information in gait analysis [2]. More versatile applications have come in the form of estimating spatio–temporal parameters, such as walking speed [3–5] or lower limb kinematics [6]. However, since the biomechanics of running is quite different from walking [7,8], i.e. the presence of double float phase, existing walking speed estimation methods could not be directly applied to the running gait. Currently, the use of inertial sensors was limited in the identification of the temporal characteristics of the running gait [9,10] and the direct quantification of accelerations during running [11,12]. To extend the utility of inertial sensors in running gait analysis, the purpose of this paper was to explore the feasibility of an inertial measurement unit in estimating running speed.

2. Methods

2.1. Running speed estimation

A shank-mounted wireless IMU (Inertia-Link®, MicroStrain, Inc., Williston, VT, USA), which consists of a triaxial accelerometer (±5 g) and a triaxial gyroscope (±600°/s), was used in the experiment to measure shank linear accelerations and angular velocities. As we only consider the shank motion in sagittal plane, the tangential and normal axes of the accelerometer are used, which are aligned with the fore-aft and longitudinal directions of the shank, respectively. The gyroscope measures the shank angular velocity in sagittal plane (Fig. 1).

Based on the measured shank angular velocity, $\omega(t)$, the instantaneous shank angle, $\theta(t)$, is calculated through a time integration,

$$\theta(t) = \int_0^t \omega(\tau)d\tau + \theta(0), \tag{1}$$

where $\theta(0)$ is the initial shank angle at the beginning of the integration. With the calculated instantaneous shank angle, a coordinate transformation is used to compute the shank horizontal and vertical accelerations in the world coordinate system, $a_x(t)$ and $a_y(t)$, using the measured shank accelerations, $a_n(t)$ and $a_t(t)$,

$$\begin{bmatrix} a_x(t) \\ a_y(t) \end{bmatrix} = \begin{bmatrix} \sin\theta(t) & \cos\theta(t) \\ \cos\theta(t) & -\sin\theta(t) \end{bmatrix} \begin{bmatrix} a_n(t) \\ a_t(t) \end{bmatrix} - \begin{bmatrix} 0 \\ g \end{bmatrix}, \tag{2}$$

* Corresponding author at: Queen's University, McLaughlin Hall, 130 Stuart Street, Kingston, ON, Canada K7L 3N6. Tel.: +1 613 533 3191.
E-mail address: qli@me.queensu.ca (Q. Li).

0966-6362/$ – see front matter © 2011 Elsevier B.V. All rights reserved.
doi:10.1016/j.gaitpost.2011.06.019

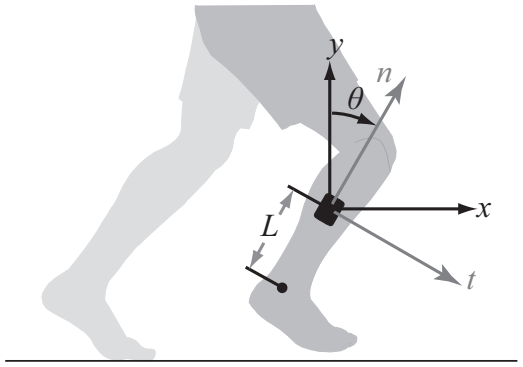

Fig. 1. Sensor configuration: an IMU is attached to the right shank in the sagittal plane on the lateral side. The normal acceleration a_n is measured along the n direction, and the tangential acceleration a_t is measured along the t direction, while the axis of gyroscope is perpendicular to the sagittal plane defined by n and t directions. The arrows indicate positive axes for the corresponding sensor measurements. The world coordinate is defined by the x and y axes, and the vertical axis y extends in a direction parallel to gravity. L is the distance between the IMU and the ankle joint.

where g is the acceleration due to the gravity. The shank horizontal and vertical accelerations are then integrated to obtain the shank instantaneous velocities in horizontal and vertical directions,

$$v_x(t) = \int_0^t a_x(\tau)d\tau + v_x(0)$$
$$v_y(t) = \int_0^t a_y(\tau)d\tau + v_y(0), \quad (3)$$

where $v_x(0)$ and $v_y(0)$ are the initial shank horizontal and vertical velocities, respectively.

A common issue of using inertial sensors in estimating running or walking speed is that the sensor bias directly affects the performance of the inertial sensor based system through integration. As shown in Eq. (3), a small sensor measurement bias will cause a bigger error in estimated velocities when the duration of integration is long. To reduce the influence of the sensor-bias related integration error, gait segmentation algorithms have been developed such that integration is performed in a short time duration. Although several gait segmentation methods [5,13] have been developed, these methods all made use of the characteristics of the measured sensor signals at different walking gait events. Since the biomechanics of running is different from walking, a new segmentation method for dividing running gait into stride cycles needs to be developed in order to minimize the integration errors. Two criteria are considered in segmenting the running sequence. First, the integration initial values of Eqs. (1) and (3) should be readily available or could be easily calculated. Second, the magnitude of the initial values should be as small as possible to minimize the calculation errors.

The gait segmentation criteria implies that the preferred starting point of integration for Eq. (1) and (3) would be the shank vertical event ($\theta = 0$, when the longitudinal direction of the shank is aligned with the direction of gravity) and the minimal shank velocity event (when the magnitude of the shank velocities reach a minimum throughout the stance phase). To identify these running gait events, we conducted a treadmill running experiment accompanied with an optical motion capture system (Optotrak 3020, Northern Digital Inc., Waterloo, Ontario, Canada). The experimental result showed that the shank vertical event occurred right after heel strike, where the shank angular velocity experienced a transition from negative to positive (Fig. 2). The minimal shank velocity event occurred just before toe off, where the horizontal shank acceleration experienced a transition from negative to positive (Fig. 2). However, the shank vertical event and the minimal shank velocity event were out of phase due to the period of double float, the integration of the angle (Eq. (1)) and the velocity (Eq. (3)) should start at different time.

An off-phase segmentation method was developed based on the above-mentioned shank kinematic characteristics. The off-phase segmentation method considers the running gait as a combination of two off-phase cycles: shank angle cycle and shank velocity cycle, as depicted in Fig. 2. The implementation of the segmentation method consists of two steps. First, the measured instantaneous shank angular velocity, $\omega(t)$, is integrated for two shank angle cycles starting from the shank vertical event to find the instantaneous shank angle, $\theta(t)$, as shown in Eq. (1). Second, the transformed shank accelerations, $a_x(t)$ and $a_y(t)$, are integrated for each shank velocity cycle between two toe off events to obtain the instantaneous shank velocities, $v_x(t)$ and $v_y(t)$, as shown in Eq. (3). As the shank velocity cycle starts from the end of the stance phase, the initial shank velocities in Eq. (3) can be calculated based on the sensor position and the shank angular velocity right before toe off, based on the assumption that the shank is approximately rotating about the ankle joint in the stance phase,

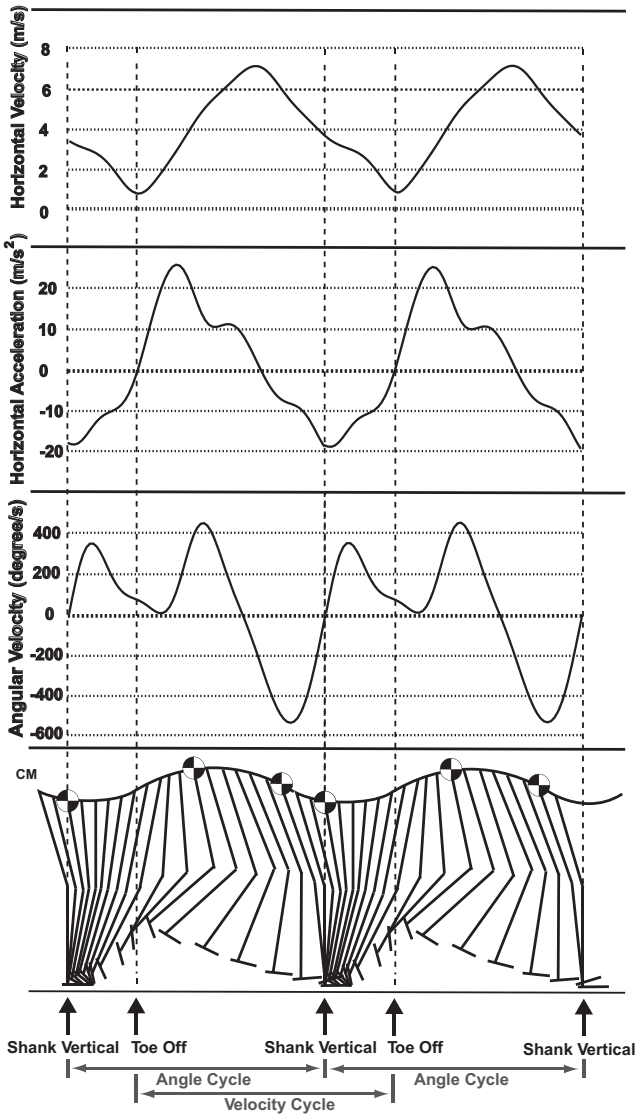

Fig. 2. Characteristics of shank velocity, acceleration and angular velocity during running. The solid curves represent the horizontal component of the shank velocity, the shank acceleration and the shank angular velocity. The shank vertical and toe off gait events can be determined by the characteristics of the shank angular velocity and shank horizontal acceleration, as indicated. The shank acceleration and angular curves were obtained from the optical motion capturing with sampling frequency 100 Hz and were processed by a second order Butterworth filter with cut-off frequency of 25 Hz.

$$v_t(0) = \omega(0) \cdot L, \quad (4)$$

$$\begin{bmatrix} v_x(0) \\ v_y(0) \end{bmatrix} = \begin{bmatrix} \cos\theta(0) \\ -\sin\theta(0) \end{bmatrix} \cdot v_t(0), \quad (5)$$

where $v_t(0)$ is the shank velocity on the tangential direction of the shank at the beginning of the shank velocity cycle and $v_x(0)$ and $v_y(0)$ are the shank horizontal and vertical velocities at the same time, respectively. $\theta(0)$ is the calculated shank angle at the toe off position. L is the distance between the IMU sensor and ankle joint (Fig. 2). Here we chosen the distance L as 0.25 m, the average value of all subjects.

In the results of the optical motion capture experiment, we also found that the raw accelerations measured by the IMU sensor experienced a constant bias. The direct consequence of the constant acceleration bias is a velocity drift in the resulting velocities, $v_x(t)$ and $v_y(t)$, during the integration process. However, the shank velocity drift can be easily corrected if the initial velocity and the end velocity are known. The initial shank velocities in each stride cycle are found according to Eqs. (4) and (5), and the same method was used to obtain the end shank velocities,

$v_{x\_calculated}(T)$ and $v_{y\_calculated}(T)$,

$$v_t(T) = \omega(T) \cdot L, \tag{6}$$

$$\begin{bmatrix} v_{x\_calculated}(T) \\ v_{y\_calculated}(T) \end{bmatrix} = \begin{bmatrix} \cos\theta(T) \\ -\sin\theta(T) \end{bmatrix} \cdot v_t(T), \tag{7}$$

where T is the period of the corresponding stride cycle defined by two adjacent toe off events.

Making use of the initial and end shank velocities, the shank velocity drifts caused by acceleration bias were compensated as (8),

$$\begin{aligned} v_{x\_corrected}(t) &= v_x(t) + \frac{v_{x\_calculated}(T) - v_x(T)}{T} \cdot t \\ v_{y\_corrected}(t) &= v_y(t) + \frac{v_{y\_calculated}(T) - v_y(T)}{T} \cdot t, \end{aligned} \tag{8}$$

where $v_x(T)$ and $v_y(T)$ are the end shank horizontal and vertical velocities from the integration of accelerations of Eq. (3). $v_{x\_corrected}(t)$ and $v_{y\_corrected}(t)$ are the instantaneous shank horizontal and vertical velocities after bias correction. The shank horizontal displacement, $s_y(T)$, and the vertical displacement, $s_y(T)$, were obtained by integrating the velocities $v_{x\_corrected}(t)$ and $v_{y\_corrected}(t)$ over an entire shank velocity cycle,

$$\begin{aligned} s_x(T) &= \int_0^T v_{x\_corrected}(t)dt + s_x(0) \\ s_y(T) &= \int_0^T v_{y\_corrected}(t)dt + s_y(0), \end{aligned} \tag{9}$$

where $s_x(0)$ and $s_y(0)$ are the initial shank horizontal and vertical displacements, respectively, which are reset to zero at the beginning of each shank velocity cycle. The stride length is computed as the net shank displacement in horizontal and vertical directions,

$$s(T) = \sqrt{(s_x(T))^2 + (s_y(T))^2}. \tag{10}$$

The vertical displacement over an entire stride cycle should be close to zero during level running. However, the vertical displacement was included in the calculation of the net displacement to accommodate the case of inclined or uneven surface running where there is a non-zero vertical displacement.

The average running speed in each stride cycle was then found by

$$V(T) = \frac{s(T)}{T}. \tag{11}$$

2.2. Experiment protocol

Treadmill running experiments were conducted to evaluate the performance of the method developed. Four male and three female subjects (age: 23 ± 2 yrs, height: 175 ± 10 cm) were recruited for the treadmill running experiments. All participants gave written consent in accordance with Queen's University General Research Ethics Board. During the experiment, the IMU was attached to the midpoint of the right shank on the lateral side. The subjects were instructed to run at five different treadmill speeds: 2.50 m/s, 2.75 m/s, 3.00 m/s, 3.25 m/s and 3.50 m/s. Each trial lasted for 90 s, and the data from the stable interval of trials were chosen for processing. However, at the speed of 3.50 m/s, the angular velocity of one subject exceeded the measuring range of the IMU (±600°/s), of which the test data was removed from the analysis for this condition.

2.3. Data analysis

All the signal processing was performed in MATLAB. On average, 5% of data loss was present in the wireless transmission. Before data processing, one-dimensional interpolation was used to reconstruct the missing data points. A second-order Butterworth low-pass filter with a cut-off frequency of 7 Hz was used to remove the noise from the raw data. For each subject, the speed estimation error at each treadmill speed was calculated as the difference between the average estimated running speed over 30 stride cycles and the preset treadmill speed. The mean estimation error (Mean) and standard deviation (SD) were determined by averaging across all subjects at each treadmill speed. A root mean squared error (RMSE) is computed as $\mathrm{RMSE} = \sqrt{\sum (V_{\mathrm{estimated}} - V_{\mathrm{actual}})^2 / N}$, where N is the number of samples in the calculation. The %RMSE was calculated as the ratio of RMSE and the preset treadmill speed. One-way ANOVA test was used to investigate the effect of the treadmill speed on the IMU running speed estimation error. With the p-values of the one-way ANOVA test larger than the significance level, 0.05, the effect of treadmill speed on the IMU running speed estimation error was considered statistically insignificant. Since the shank segment is like a cylinder, the sensor cannot be attached to the lateral side of the shank perfectly aligned with the sagittal plane. Any misalignment between the sensor axes and the sagittal plane would result in smaller measurement than actual value. In order to analyze the error from such misalignment, a sensor attachment sensitivity test was conducted, where an angle of 10° was simulated between the sensor axes and the sagittal plane. The estimation result was compared to that without the misalignment.

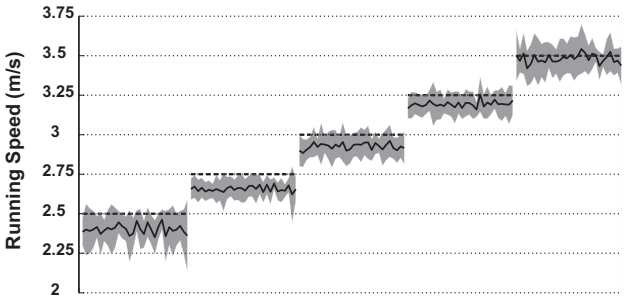

Fig. 3. Stride-by-stride running speed estimation results. For each running speed, thirty strides from the steady running period of each subject were used in the analysis. The average and the standard deviation of the estimates at each stride were calculated across all subjects. The dashed lines indicate the constant reference treadmill speeds. The solid curves are the average estimated stride-by-stride running speeds. The shadow regions are the average estimated running speed ± one standard deviation, indicating the inter-subject variability. The estimation results for 3.50 m/s running trials were from six subjects.

3. Results

The proposed algorithm was capable of accurately estimating running speed. Slight underestimation of the running speed was observed in the estimation results. Results of the running speed estimation method, gathered from all subjects at each treadmill speed, are shown in Fig. 3.

Table 1 summarizes the estimation errors of the proposed running speed method. The overall %RMSE is 4.10% for all subjects. One-way ANOVA test showed that the running estimation error presented no significant difference in treadmill speeds ($p = 0.83$). The sensor attachment sensitivity test on running experimental data showed a 10° misalignment would result in as much as 8% reduction of estimated running speed.

4. Discussion

The proposed method slightly underestimated the running speed and presented some inter-subject, as well as stride-to-stride variability (Fig. 3). One explanation to the underestimation could be the misalignment of inertial sensor axes. As shown in the sensor attachment sensitivity test, the misalignment of the sensor axes with sagittal plane could eventually lead to an underestimation of the running speed. Another potential source for the underestima-

Table 1
Treadmill running speed estimation errors.

	Treadmill speed (m/s)					Overall %RMSE
	2.50 [a]	2.75 [a]	3.00 [a]	3.25 [a]	3.50 [b]	
Abs. mean ± SD	0.11 ± 0.03	0.10 ± 0.03	0.08 ± 0.02	0.08 ± 0.02	0.09 ± 0.02	4.10%
%RMSE	5.85%	4.25%	3.73%	2.87%	3.10%	

[a] Analysis is based on the data collected from seven subjects.
[b] The errors for 3.50 m/s running trials were based on the estimation results of six subjects.

tion could be caused by the error in estimating the initial shank velocity. The initial shank velocity was calculated as the product of the measured shank angular velocity and the distance between the IMU sensor and the ankle joint, for which the sensor-to-ankle joint distance was chosen as the rotation arm and considered as a constant based on the average value from all subjects. However, since heel lift occurs before toe off, the shank segment theoretically does not rotate about the ankle joint, and the sensor-to-ankle distance is shorter than the actual rotation arm. As it is quite difficult to accurately measure the rotation arm at toe off, our estimated initial shank velocity was only a rough approximation. The use of generic value of L also could account for some of the inter-subject variability observed in the results. The stride-to-stride variability of the estimated speed is within the range of natural variation in human stride length and timing during running. Several studies [15,16,14] have investigated these variations in trained athletes running on treadmills. Craib et al. reported that stride length can vary up to 2.50% at approximately the same speed range used in this study [14]. It is also speculated that this value would increase in untrained runners, such as those that participated in this study.

Previous work on IMU-based running gait analysis mostly focused on using inertial sensor for identifying gait events [9] or gait symmetry [10]. Very few studies and commercial products have been reported on using inertial sensor in estimating spatio-temporal parameters, such as running speed estimation. Hausswirth et al. conducted a study of using an accelerometer-based foot-mount running analysis system (RS800sd, Polar®, Kempele, Finland) to estimate running speeds. With a subject-by-subject calibration, the system achieved an error of 4.9% in treadmill running experiments [17]. Our proposed running speed estimation method achieved a slightly better performance while no subject-by-subject calibration is required. Since the algorithm used in Polar® RS800sd was proprietary, and most of the running speeds tested in Hausswirth's were higher than those in our study, we could not perform a direct comparison.

Identifying gait characteristics from inertial sensor measurements is the key in developing effective gait speed estimation methods for walking and running. In previous inertial sensor based walking speed estimation study [5], an inverted pendulum model has been used to model the stance phase of walking gait. The inverted pendulum model suggested that at the shank vertical event the body center of mass reached its highest point and potential energy reaches a maximum. However, in running gait, the inverted pendulum model does not apply due to the period of double float. In contrast to inverted pendulum, the running gait behaves as a spring-mass system [18–20]. The spring-mass system models the human body as a combination of a mass (upper body) and a spring (lower limbs). Starting from heel strike, the muscle of the stance leg contracts as a spring, which virtually absorbs the energy delivered by the body mass during the drop, and at the same time the shank changed the rotation direction at the shank vertical event (Fig. 2). The lowest position of the body center of mass occurs when the leg is fully contracted, after which the stance leg starts to release the energy stored in the muscle and push the body to move upward and forward. However, due to the bending of the knee joint, the body acceleration is not observed on the shank. Right after toe off event, the shank starts to accelerate following the motion of the body (Fig. 2), and then pass the body reaching the next heel strike. The off-phase segmentation for the shank angle and the shank velocity is beneficial in two aspects. First, the shank vertical event occurs at the heel strike when the shank moves forward at a high speed and the rotation center of the shank is unknown. The initial shank velocity is difficult to be accurately calculated with only the shank angular velocity and acceleration information. Second, at the toe off event the shank velocity is the lowest of the entire running gait cycle, which help reduce the error from the calculation of initial shank velocity associated with the estimation of the rotation arm. Moreover, the shank rotates about the ankle joint before toe off, which makes the calculation of the initial shank velocity possible (Eqs. (4) and (5)).

One limitation of this study was the selection of running speeds, which was limited by the IMU sensor used in the experiment. Inertia-Link® is capable of measuring angular velocity in a range of $\pm 600^{\circ}/s$; in the experiment we found that at the highest treadmill running speed (3.50 m/s) the shank angular velocity of one subject exceeded the measuring range. As the pattern of lower limb motion in running and sprinting is very similar [8], the proposed method will most likely work for higher running speeds. However, the applicability of the proposed method in sprinting requires further experimentation using an IMU with a larger measurement range.

5. Conclusion

This study proposed a novel shank-mounted IMU method to estimate running speed. Multiple speeds treadmill running experiments demonstrated the feasibility of using an IMU in estimating running speeds. With further development, inertial sensor could be potentially used as a low-cost alternative to the optical motion capture system in running biomechanics research. In addition, the ambulatory capability of the inertial sensor also helps bring the running gait analysis out of the lab environment where more natural movements are expected to be performed.

Acknowledgement

I would like to gratefully acknowledge the support from NSERC discovery grant.

Conflict of interest statement

No author of this paper has a conflict of interest, including specific financial interests, relationships, and/or affiliations relevant to the subject matter or materials included in this manuscript.

References

[1] Higginson B. Methods of running gait analysis. Current Sports Medicine Reports 2009;8(3):136–41.
[2] Kavanagh JJ, Menz HB. Accelerometry: a technique for quantifying movement patterns during walking. Gait and Posture 2008;28(1):1–15.
[3] Aminian K, Najafi B, Bula C, Leyvraz PF, Robert P. Spatio-temporal parameters of gait measured by an ambulatory system using miniature gyroscopes. Journal of Biomechanics 2002;35(5):689–99.
[4] Hartmann A, Murer K, de Bie RA, de Bruin ED. Reproducibility of spatio-temporal gait parameters under different conditions in older adults using a trunk tri-axial accelerometer system. Gait and Posture 2009;30(3):351–5.
[5] Li Q, Young M, Naing V, Donelan JM. Walking speed estimation using a shank-mounted inertial measurement unit. Journal of Biomechanics 2010;43(8):1640–3.
[6] Liu T, Inoue Y, Shibata K. Development of a wearable sensor system for quantitative gait analysis. Measurement 2009;42(7):978–88.
[7] Mann RA, Hagy J. Biomechanics of walking, running, and sprinting. American Journal of Sports Medicine 1980;8(5):345–50.
[8] Novacheck TF. The biomechanics of running. Gait and Posture 1998;7(1):77–95.
[9] Lee JB, Mellifont RB, Burkett BJ. The use of a single inertial sensor to identify stride, step, and stance durations of running gait. Journal of Science and Medicine in Sport 2010;13(2):270–3.
[10] Lee JB, Sutter KJ, Askew CD, Burkett BJ. Identifying symmetry in running gait using a single inertial sensor. Journal of Science and Medicine in Sport 2010;13(5):559–63.
[11] Lafortune MA. Three-dimensional acceleration of the tibia during walking and running. Journal of Biomechanics 1991;24(10):877–9.
[12] Zijlstra W, Hof AL. Assessment of spatio-temporal gait parameters from trunk accelerations during human walking. Gait and Posture 2003;18(2):1–10.

[13] Sabatini AM, Martelloni C, Scapellato S, Cavallo F. Assessment of walking features from foot inertial sensing. IEEE Transactions on Biomedical Engineering 2005;52(3):486–94.
[14] Craib M, Caruso C, Clifton R, Burleson C, Mitchell V, Morgan D. Daily variation in step length of trained male runners. International Journal of Sports Medicine 1994;15(2):80–3.
[15] Belli A, Lacour J, Komi P, Candau R, Denis C. Mechanical step variability during treadmill running. European Journal of Applied Physiology and Occupational Physiology 1995;70(6):510–7.
[16] Danion F, Varraine E, Bonnard M, Pailhous J. Stride variability in human gait: the effect of stride frequency and stride length. Gait and Posture 2003;18(1):69–77.
[17] Hausswirth C, Le Meur Y, Couturier A, Bernard T, Brisswalter J. Accuracy and repeatability of the Polar® RS800sd to evaluate stride rate and running speed. International Journal of Sports Medicine 2009;30(5):354–9.
[18] Blickhan R. The spring-mass model for running and hopping. Journal of Biomechanics 1989;22(11–12):1217–27.
[19] Dalleau G, Belli A, Bourdin M, Lacour JR. The spring-mass model and the energy cost of treadmill running. European Journal of Applied Physiology and Occupational Physiology 1998;77(3):257–63.
[20] Geyer H, Seyfarth A, Blickhan R. Spring-mass running: simple approximate solution and application to gait stability. Journal of Theoretical Biology 2005;232(3):315–28.